Energy & Environmental Science

REVIEW

View Article Online
View Journal | View Issue

Cite this: *Energy Environ. Sci.*, 2015, **8**, 776

Polyoxometalate-functionalized nanocarbon materials for energy conversion, energy storage and sensor systems

Yuanchun Ji,[a] Lujiang Huang,[a] Jun Hu,[a] Carsten Streb*[b] and Yu-Fei Song*[a]

Received 27th November 2014
Accepted 7th January 2015

DOI: 10.1039/c4ee03749a

www.rsc.org/ees

Composites based on polyoxometalates (POMs) and nanostructured carbon such as carbon nanotubes (CNTs) or graphene have attracted widespread attention as they combine the unique chemical reactivity of POMs with the unparalleled electronic properties of nanocarbons. The exceptional properties of these composites have been employed in catalysis, energy conversion and storage, molecular sensors and electronics. Herein, we summarize the latest progress in POM/CNT and POM/graphene nanocomposites with a focus on energy materials for water splitting and fuel cells, composite electrode materials for batteries and supercapacitors as well as composites for environmental pollutant sensing. Current applications are critically assessed and promising future target systems are discussed.

1. Introduction

Over the last decade, scientists and politicians worldwide have acknowledged that there is an increasingly urgent demand for sustainable energy conversion and energy storage solutions. To this end, functional materials are required that allow the continuous and efficient conversion of solar or electrical energy into storable energy, *e.g.* in the form of chemical bonds (*e.g.* H_2).[1–5] Recently, composite materials based on polyoxometalates (POMs) and nanocarbon including carbon nanotubes (CNTs) and graphene have shown great potential to meet the challenges in electrocatalysis, energy storage, sensor devices and other cutting-edge technologies.[6–8]

Polyoxometalates are anionic molecular metal oxides based on early, high-valent transition metals (*e.g.* V, Mo, W) with outstanding versatility in research fields including catalysis, energy conversion and molecular electronics.[9–11] Nanocarbon materials, including carbon nanotubes (CNTs) and graphene, have been used in energy conversion, electrochemistry, and electronics as they combine unique nano-sized structures with exceptional electronic and spectroscopic features.[12–17] However, when systems for electron transfer are developed, it is critical to electrically "wire" the POMs to conductive substrates, ideally at

[a]*State Key Laboratory of Chemical Resource Engineering, Beijing University of Chemical Technology, 100029 Beijing, P. R. China. E-mail: songyufei@hotmail.com; songyf@mail.buct.edu.cn*

[b]*Institute of Inorganic Chemistry I, Ulm University, Albert-Einstein-Allee 11, 89081 Ulm, Germany. E-mail: carsten.streb@uni-ulm.de*

Yuanchun Ji received his BSc degree in 2012 from Beijing University of Chemical Technology. He is currently in a Master program under the supervision of Prof. Yu-Fei Song at the same University (2012–2015). His research work mainly focuses on the polyoxometalate-containing electrode materials. In 2014, he worked for three months with Prof. Carsten Streb (Ulm University) as an exchange student funded by the German Academic Exchange Service (DAAD).

Lujiang Huang received his BSc degree in Applied Chemistry in 2012 and he is going to finish his master program in June 2015. He studies at Beijing University of Chemical Technology under the supervision of Prof. Yu-Fei Song. His research interests are the development of nanocomposites based on the polyoxometalate/nanocarbon materials for energy storage and conversion.

molecular dispersion so as to maximize the electron-transfer activity within the material and to the external circuit. This approach is required as POMs are typically salts with negligible conductivity[18] making them unsuitable for direct use in electrical energy conversion/storage or amperometric sensing. In addition, it was shown that molecular dispersion of POMs on nanocarbons such as graphene significantly modifies the electronic structure of the cluster, meaning that device performance needs to be investigated and understood on the molecular level.[19] Therefore, in recent years, researchers have started to harness the synergistic effects between POMs and nanocarbons by developing molecular composites to address the pressing global energy challenges.[20,21]

Based on recent advances in the chemical modification of nanocarbons, new materials are now available that combine high surface area and electrical conductivity with the ability to intimately link reactive species such as POMs to the nanocarbon surface through a range of intermolecular or covalent interactions. This allows a molecular dispersion of POMs on the nanocarbon, so that each individual cluster anion can be electronically addressed and can be involved in energy and electron transfer processes.[22,23] In this account, we focus on the application-driven development of POM/nanocarbon composites with use in energy conversion, energy storage, electrocatalysis and chemical/biochemical sensing. A table of abbreviations is given at the end of the review.

2. Preparation of POM/nanocarbon composite materials

Two main pathways for the preparation of the POM/nanocarbon composites can be identified, their main advantages and disadvantages together with potential future directions are described below.

2.1 Covalent functionalization routes

Covalent attachment of POMs to nanocarbons requires access to stable organo-functionalized POMs. This by itself is often synthetically challenging and typical functionalization groups are restricted to organo-functionalized alkoxides, silanes, phosphonates and imides.[24,25] Often, one organic functionalization group can only be linked to one specific cluster type, so that currently, no unified functionalization strategy exists. In addition, the functionalization step can be carried out during the actual cluster assembly (*direct functionalization*) or after the cluster has been synthesized (*post-functionalization*), making it more difficult for the non-expert to choose the ideal synthetic approach.[24,25] Further, the bonding between POM and functional organic group is often relatively weak so that the application range is seriously hampered. Thus, the development of general functionalization routes leading to stable, long-lived

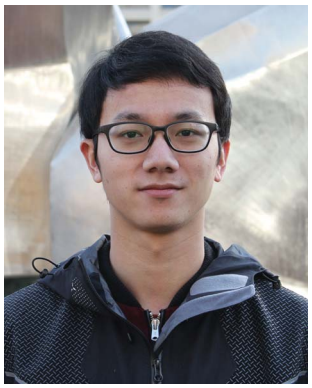

Jun Hu received his BSc Degree in 2012 from Beijing University of Chemical Technology. He is currently a PhD student at Beijing University of Chemical Technology under the supervision of Prof. Yu-Fei Song. His research interests involve the development of polyoxometalate-based multifunctional materials for energy applications.

Carsten Streb studied chemistry at TU Kaiserslautern (Germany). He then undertook a PhD with Prof Lee Cronin at the University of Glasgow (Scotland, UK) focusing on inorganic host–guest systems and porous framework materials (POMOFs). Subsequently, he did a postdoc at the University of Glasgow and James Watt Nanofabrication Centre, developing nanostructured semiconductors. In 2009, Carsten started his independent research as a Liebig-Fellow at the Friedrich-Alexander-University Erlangen-Nuremberg (Germany). In 2013 he became Professor of Inorganic Chemistry at Ulm University (Germany). His current research interests are novel synthetic routes to functional molecular metal oxides for sustainable energy conversion and storage.

Dr Yu-Fei Song received his PhD (2002) Degree from Shanxi University. After postdoc research in Leiden University (2002–2004, The Netherlands), Max-Planck Institute of Bio-inorganic Chemistry (2004–2005, Germany), and The University of Glasgow (2005–2008, UK), he joined Beijing University of Chemical Technology (BUCT) in Sep, 2008 as a full professor. He is currently holding a professor position in the State Key Laboratory of Chemical Resource Engineering, BUCT. His research interests mainly focus on the polyoxometalate-based new molecular assemblies and multifunctional materials. He has published over 90 research papers in SCI journals. In 2009, he was selected to be one of the members in the "New Century Outstanding Talent scheme of the Ministry of Education". In 2012, he was supported by "National Science Foundation for Excellent Young Scholars".

organic–inorganic hybrid materials is one major challenge of modern POM research.

To date, the typical approaches used to functionalize nanocarbons with POMs employ POM clusters where a pendant amine has been introduced *via* the functional group. This moiety can then be linked to oxidized nanocarbons through the formation of amides.[26]

2.2 Non-covalent functionalization routes

Non-covalent bonding can be achieved using a range of intermolecular interactions between POMs and nanocarbons.

(1) Electrostatic interactions: The current state-of-the-art is the use of electrostatic interactions to attach anionic POMs to positively charged nanocarbons. Cationic functionalization of nanocarbons can be achieved by (a) covalent attachment of cations, typically to oxidized CNTs or graphene where –OH and –COOH groups are available for further functionalization[8] and (b) through intermolecular interactions, *e.g.* van der Waals-interactions[27] or π–π-interactions which are used to attach cationic species to the nanocarbon surface.[28]

(2) π–π-interactions: When an extended aromatic system (*e.g.* pyrene) is covalently attached to a POM, this hybrid molecule can be linked to nanocarbons through π–π stacking interactions.[20,29] As describe above, this approach, however, requires access to organo-functionalized POMs which in itself is still challenging, see Section 2.1.

(3) Layer-by-layer (LbL) assembly: LbL assembly can be achieved by repeatedly stacking POMs and nanocarbons using wet-chemical deposition methods. By cationic modification of the nanocarbon, strong electrostatic interactions can be used to stack the alternating POM and nanocarbon layers.[30] It should be noted that the LbL deposition technique gives only access to layered structures where the electronic interaction and dispersion of POM and nanocarbon might not be ideal. However, the simplicity and variability of this preparation method has made it one of the most commonly used techniques for the fabrication of energy conversion devices.[31]

(4) In addition to these well-known assembly methods for POM/nanocarbon composites, electro-assisted or photo-assisted assembly have also be used to fabricate POM/nanocarbon composite materials.[32–34] For example, Wu *et al.*[33] have successfully fabricated a nanocomposite through a SiW_{12}-catalyzed electrochemical reduction where SiW_{12} transfers electrons from the electrode to GO (graphene oxide), giving rGO (reduced graphene oxide). SiW_{12} is then adsorbed on the rGO nanosheets and a highly dispersed, porous SiW_{12}/rGO nanocomposite is obtained. The high porosity makes the material interesting as a cathode material for lithium ion batteries and high specific capacity (275 mA h g^{-1}, 1.7 times the capacity of pure SiW_{12}) was found.

3. Applications of POM/nanocarbon composites

Based on their general redox-activity, POMs linked to nanocarbons can be employed for a wide range of electron transfer and storage processes. Currently, most research in POM/nanocarbon composites has been focused on electrocatalysts, electrochemical energy storage and environmental pollutant sensing. The following sections will review these fields and provide an outlook at the challenges and future perspectives of the area.

3.1 Electrocatalysis

The high redox-activity of POMs makes them ideal for the catalytic transfer of electrons to or from a substrate (*i.e.* reductive or oxidative electrocatalysis). This is particularly appealing for the development of multi-electron transfer reactions which are typically hampered by high overpotentials leading to low overall conversion efficiencies. POMs are ideal candidates to address this challenge as they can be chemically modified with highly redox-active metals (*e.g.* Co, Mn, Ru). Thus, technologically relevant electrocatalysts for the splitting of water into oxygen and hydrogen[35,36] as well as for oxidation and reduction reactions in fuel cells become accessible.[37]

3.1.1 Water oxidation. Water oxidation is generally considered the more challenging half-reaction of the water-splitting process. Often, high over-potentials are observed, even when noble metals such as platinum (overpotential: *ca.* 0.8 V) are employed as electrodes.[38] To overcome this obstacle, highly functionalized POM-based water oxidation catalysts (WOCs) functionalized with redox-active metals such as Co and Ru have been developed.[39,40] In 2010, Bonchio *et al.*[20] electrostatically assembled a prototype POM-WOC, $(M_{10}[Ru_4(H_2O)_4(\mu\text{-}O)_4(\mu\text{-}OH)_2(\gamma\text{-}SiW_{10}O_{36})_2]$ $(= M_{10}Ru_4(SiW_{10})_2$, $M = Cs^+, Li^+))$ on multi-walled carbon nanotubes (MWNTs) as the conductive substrate to form an active water oxidation electrocatalyst (Fig. 1). The nanostructured composites were used as anodes in a water-splitting device and water oxidation with over-potentials as low as 0.35 V and TOFs approaching those of the cluster in

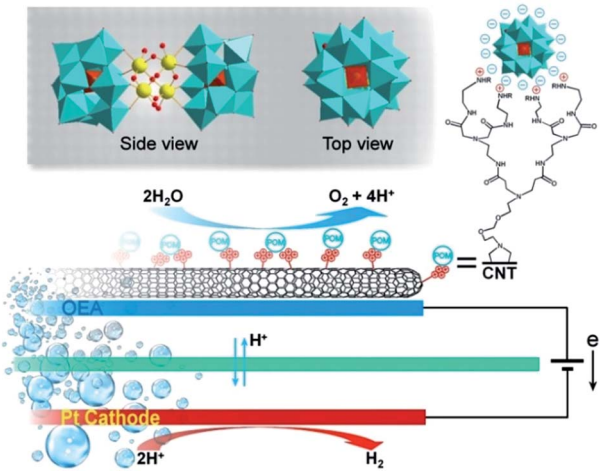

Fig. 1 General scheme for a water-splitting electrocatalytic cell with the integrated nanostructured oxygen-evolving anodes (OEAs) based on polyanionic ruthenium-containing POMs.[20] The POM used is $[Ru_4(H_2O)_4(\mu\text{-}O)_4(\mu\text{-}OH)_2(\gamma\text{-}SiW_{10}O_{36})_2]$. Colour scheme: blue: W, brown: SiO_4^{4-}, yellow: Ru, red: O.

homogeneous solution (up to 300 h^{-1}).[41] The example illustrates that the high reactivity of the molecular WOC can be retained whilst immobilizing the cluster on the electrically conducting MWNTs enables integration into a technological device.

Following this initial breakthrough, Bonchio *et al.*[42] noted that the binding of the POM to the CNT was still not optimal and therefore devised new covalent and non-covalent approaches to functionalize the CNTs with cations (Fig. 2). In one example, pyrene-based cationic species were linked to CNTs by π–π interactions using an innovative, solvent-free microwave procedure, thereby eliminating hazardous volatile organic solvents and also accelerating reaction time and maximizing product yields. The cationic CNTs obtained showed high binding affinity for the anionic POM-WOCs and the formation of nanostructured composite surfaces was observed upon drop-casting the composite on electrode surfaces, giving access to high surface-area electrocatalysts.[42]

Compared with carbon nanotubes, graphene is highly stable, conductive and has a large surface area to volume ratio, making it ideal for electrochemical applications involving immobilized catalysts. Significant increases in electrocatalytic performance have been observed when graphene is used as the catalyst support.[43] In 2013, Bonchio *et al.*[8] developed a highly robust water oxidation electrocatalyst by combining their Ruthenium-based POM WOC $Ru_4(SiW_{10})_2$ with functionalized graphene. The graphene was covalently functionalized with organic, hydrogen-bonding cations, allowing the anchoring of $Ru_4(SiW_{10})_2$ by a combination of electrostatic and hydrogen-bonding interactions (Fig. 3). The resulting composite material displays oxygen evolution at overpotentials as low as 300 mV at neutral pH with negligible loss of performance after 4 h testing. The authors suggested that the high catalytic activity and stability is due to the non-invasive and highly dispersed surface modification of the graphene, which enables electron transport and accumulation across the extended π-bond network. Also in 2013, Hill *et al.*[44] studied a similar Ru-containing POM/rGO composite using electrochemical analyses; here, graphene was electrochemically deposited on a glassy carbon or ITO electrode from a graphene oxide suspension; subsequently, the POM was immobilized electrostatically. The composite showed excellent catalytic activity and high stability for the water oxidation reaction under neutral pH conditions, particularly in the presence of 1.0 M $Ca(NO_3)_2$, with a moderate over-potential of 0.35 V. These initial results show the huge potential of the synergism between the Ru-containing POMs as catalysts and graphene as conductive support.

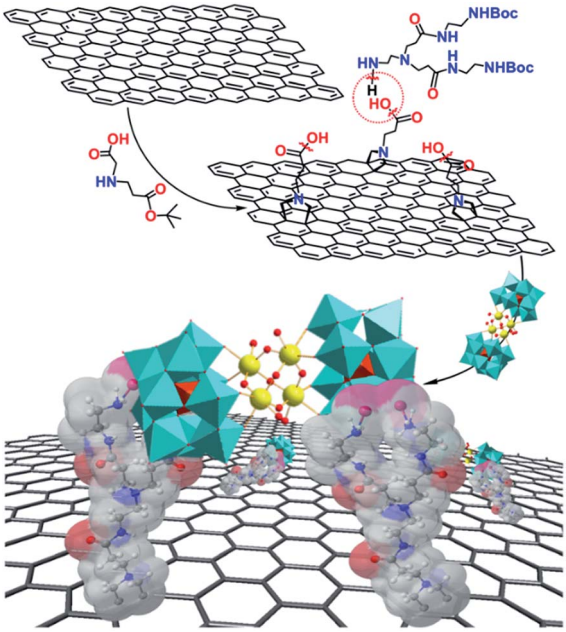

Fig. 3 Synthesis of cationic graphene nano-platforms supporting $Ru_4(SiW_{10})_2$. Graphene is covalently functionalized with organic cations, which then bind $Ru_4(SiW_{10})_2$ through electrostatic interactions.[8]

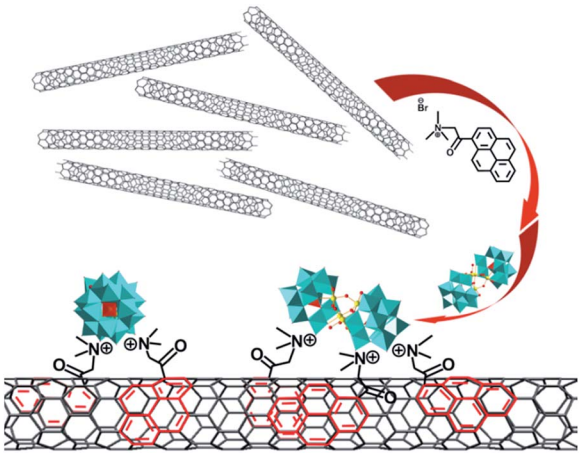

Fig. 2 Schematic illustration of the CNT-bound POM catalyst: the CNTs are functionalized with an amphiphilic cationic pyrene derivative by π–π stacking; the anionic $Ru_4(SiW_{10})_2$ is subsequently immobilized by electrostatic interactions.[42]

In summary, the conceptual viability of POM/CNT and POM/graphene composites for efficient water oxidation catalysis has been established. The next steps require the development of systems where the costly noble metal catalysts are replaced by earth abundant materials whilst retaining high catalytic activity. One promising POM compound towards this end is a cobalt-based POM-WOC, $[Co_4(H_2O)_2(PW_9O_{34})_2]^{10-}$.[45] This highly active WOC (turnover frequency >5 s^{-1}) is based on earth-abundant metals only and when combined with nanocarbons could be a highly competitive heterogeneous electrocatalytic WOC.

3.1.2 Methanol oxidation. The electrocatalytic oxidation of methanol using precious metal catalysts has attracted great interest as methanol is used as energy carrier and electron donor in direct methanol fuel cells (DMFCs).[46] Current systems typically employ noble metals, often platinum, as the anode material for the electrocatalytic methanol oxidation in DMFCs. The electro-oxidation of methanol on Pt is complicated by the formation of chemisorbed reaction intermediates such as CO, COH, and HCO which lead to catalyst poisoning.[47] The incorporation of POMs into the electrode materials is one approach

to address this: the clusters can be used as electrooxidation catalysts as well as electron and proton relays with remarkable chemical and thermal stability, allowing the long-term use of POM-modified electrodes at temperatures >100 °C, thereby lowering the accumulation of catalyst poisons on the metal surface. However, it should be noted that most current systems still employ noble metal particles as active oxidation catalysts. Here, we will discuss the current catalytic systems for methanol oxidation electrodes and identify the most critical challenges which need to be addressed to advance the field.

In 2006, Chen *et al.*[48] reported a new catalyst support based on CNTs modified with Keggin-type POMs $H_3PMo_{12}O_{40}$ (= H_3PMo_{12}), and spontaneous and strong chemisorption of the POMs on the CNTs was observed. The composite was used as a redox-active support for highly dispersed Pt and Pt–Ru electrocatalysts which were deposited using electrodeposition methods. Catalytic tests showed that the combination of the unique electrical properties of the CNTs and the excellent redox properties and the high protonic conductivity of the POMs resulted in increased current densities, high specific activity and improved cycle stability compared with non-POM-modified systems. These results provided the first experimental evidence that POM-modified CNTs are viable catalyst supports for DMFCs (Fig. 4).

In 2008, Kim *et al.*[49] proposed a Pt@POM/CNT tri-component composite for methanol oxidation which allows the reduction of the amount of noble metals used: the POM anion PMo_{12} was chemically impregnated into Pt-supported carbon nanotube (Pt/CNT) catalysts *via* a colloidal method. This composite exhibited superior Pt-based mass activities with improved stability in the methanol oxidation, as compared with Pt/CNT, Pt/C, and Pt–Ru/C. These findings demonstrate that similar tri-component systems might be developed further, and can give access to materials where higher activity per gram of noble metal is observed, making the materials attractive for commercial developments. However, still, more insight into the long-term performance of these systems compared with standard reference systems is required.

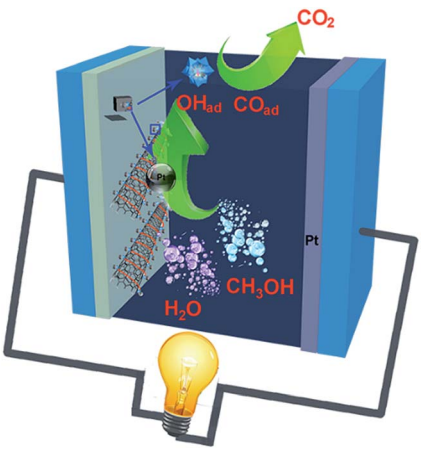

Fig. 4 Electrochemical reactions in a direct methanol fuel cell functionalized with PMo_{12}-modified CNTs. The PMo_{12}/CNTs were used to support highly dispersed Pt and Pt–Ru electrocatalysts formed by electrodeposition. The presence of POMs was shown to effectively reduce catalyst poisoning and increased the catalytic performance.[48]

A different approach to optimize methanol oxidation performance is to increase the active surface area of the metal catalysts. This also allows a reduction of the overall amount of noble metals employed. In 2009, it was shown that POMs can be used to this end: Guo *et al.*[50] developed the mixed-metal composite Pt–Sn@PMo_{12}/CNT using a microwave-heated polyol process. The authors report that the presence of PMo_{12} resulted in homogeneously deposition of the Pt and Sn particles on the CNTs. The electrochemical surface area of the Pt–Sn@PMo_{12}/CNTs catalyst was significantly higher compared with several reference systems. This is attributed to the smaller size and more uniform distribution of Pt particles, as well as the presence of PMo_{12} which might stabilize small Pt particles during their formation; in addition, it is suggested that PMo_{12} acts as co-catalyst for the methanol oxidation. The authors also showed that their system addresses the issue of catalyst poisoning, since PMo_{12} and Sn promote the oxidation of carbon-based intermediates during the methanol electro-oxidation thereby enhancing the electrocatalytic activity.

An innovative approach to deposit small Pt nanoparticles on CNTs for methanol oxidation was presented by Zhang *et al.*:[21] the group used the *in situ*-photochemically reduced Keggin cluster $H_3PW_{12}O_{40}$ (= H_3PW_{12}) as a redox mediator to reduce the Pt^{II} precursor and also as a linkage group to stabilize the nanoparticles on the CNT surface (Fig. 5). The composite showed significantly increased electrocatalytic activity towards methanol oxidation compared with traditional Pt/C catalysts and other related Pt/CNT reference systems. In addition, the onset and peak potential for methanol oxidation by Pt@POMs/CNTs showed a shift to lower values relative to the Pt/C reference catalyst, indicating the enhanced oxidation performance of the composite. A similar photochemical assembly route was used by Zhang *et al.*[22] to deposit Pt or Pd NPs, on GO (Fig. 5) using PW_{12} to photochemically reduce the Pt^{II} or Pd^{II} precursors as well as the GO and simultaneously encapsulate and bind the NPs to the rGO surface. The composites showed significantly increased electrocatalytic methanol and formic acid oxidation activity compared with traditional carbon black-based catalysts. The studies highlight the multi-functionality offered by the POM as reductant, encapsulating agent and co-catalyst which is associated with its intrinsic redox-activity.

The group of Jiang *et al.*[51] focused on new approaches to electrostatically stabilize POM anions on cationic CNTs using the methods of self-assembly: to this end, CNTs functionalized with cationic, protonated chitosan (CS) were used to strongly bind the Keggin anions PMo_{12} and PW_{12} (Fig. 6). The procedure introduces homogenous surface functional groups with no detrimental effect on the CNT structure and can be carried out at room temperature without use of corrosive acids. Deposition of Pt–Ru NPs on these composites using an impregnation route gave particles with uniform spatial distribution and smaller particle size compared with materials prepared using conventional procedures. Electrochemical MeOH oxidation tests showed a shift of the oxidation waves to more negative

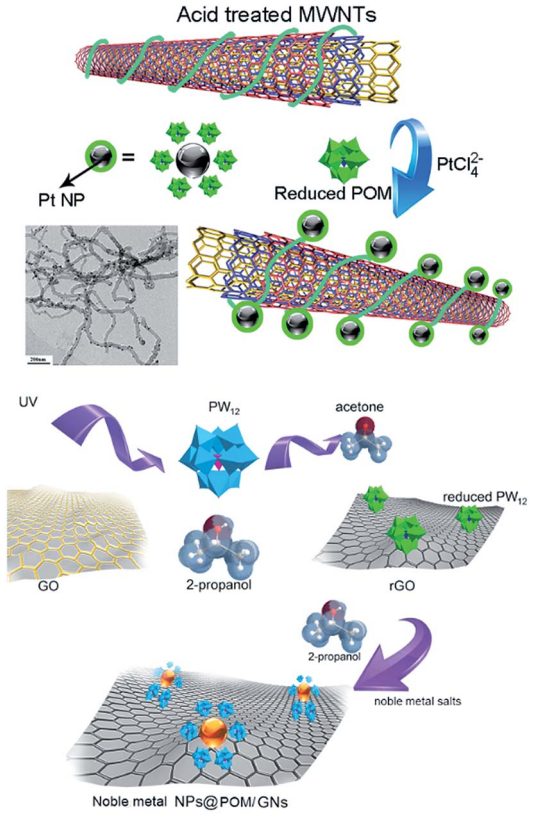

Fig. 5 (Top) Formation of Pt@POM/CNT composite electrocatalysts. The POM (PW_{12}) is photochemically reduced using UV-irradiation (electron donor: 2-propanol); the reduced PW_{12} is combined with MWNTs and H_2PtCl_4, giving the Pt@POM/CNT composite.[21] Inset: TEM image of Pt@POM/CNT composite. Reproduced from ref. 21 with permission of Elsevier Publishers. (Bottom) Preparation of the tri-component metal NPs@POM/GNs composites. (1) Photoreduction of PW_{12} by 2-propanol under UV-irradiation; (2) GO reduction by reduced-PW_{12}, giving PW_{12}/rGO composites; (3) photoreduction of the PW_{12}/rGO composites by 2-propanol, giving reduced-PW_{12}/rGO; (4) reduction of noble metal salts by the reduced-PW_{12}/rGO, giving noble metal NPs@POM/GNs.[22]

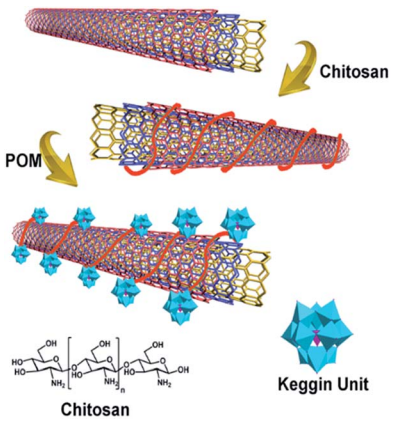

Fig. 6 Schematic diagram of the functionalization of CNTs with chitosan and Keggin-type POMs (PMo_{12} and PW_{12}). The combination of the cationic chitosan (schematically shown as a red line) and the anionic Keggin units is achieved through electrostatic interactions.[51]

potential, and higher current densities for both Pt–Ru@PMo_{12}/CS/CNTs and Pt–Ru@PW_{12}/CS/CNTs compared with standard reference systems was observed. A related study by Yuan *et al.*[52] investigated Pt–Ru@PMo_{12}/MWNT and Pt@PMo_{12}/MWNT methanol oxidation electrocatalysts and also reported that the presence of the POM induces smaller size and higher dispersion of the Pt–Ru (or Pt) NPs. In addition, the composites showed high CO tolerance under typical operating conditions, making the materials interesting for technological deployment under industrial conditions.

In summary, current studies demonstrate that POM-modified nanocarbon electrodes can provide multiple benefits to modern methanol oxidation electrodes, particularly in the fields of metal nanoparticle deposition and stabilization, improved catalyst poison resistivity and reduced usage of noble metals. However, one major challenge in the field is still the development of low overpotential electrodes for methanol oxidation which do not use noble metal catalysts. Therefore, access to highly active POM-based methanol oxidation catalysts which could act on a molecularly dispersed level might provide a facile and promising route to earth-abundant, technologically relevant materials. As such, many of the concepts described earlier in the field of POM/nanocarbon water oxidation catalysis might indeed be transferred to this related application.

3.1.3 Oxygen reduction. Besides MeOH oxidation, fuel cells also require efficient oxygen reduction catalysts to overcome the issues related with excessive overpotentials.[53,54] Typically, noble metals such as Pt and Pd are the catalyst of choice despite their high cost.[55,56] Thus, considerable efforts are underway to replace today's catalysts with earth-abundant materials. In this section, a series of POM/noble metal/nanocarbon composites as oxygen reduction catalysts will be critically discussed.

In 2010, Jiang *et al.*[57] introduced a Pd@POM/PDDA/MWNT electrocatalyst (Fig. 7), with high potential as effective non-Pt catalyst for the oxygen reduction reaction (ORR) in fuel cells. To this end, MWNTs were functionalized with poly(diallyldimethylammonium chloride) (= PDDA), forming positively charged PDDA–MWNTs. POMs (PW_{12}) were electrostatically attached to the MWNTs followed by reductive Pd deposition. The composite material possesses a significantly higher amount

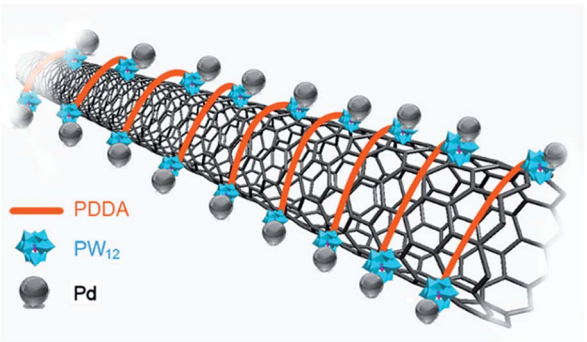

Fig. 7 Self-assembly of Keggin-type POMs (PW_{12}) on PDDA-functionalized MWNTs *via* electrostatic interactions and subsequent deposition of Pd NPs on POMs assembled PDDA–MWNTs by reductive chemical deposition.[57]

of metallic Pd compared with Pd/acid treated-MWNTs, which indicates that it has a weaker oxophilicity, and it would facilitate desorption of O_{ads}; this is a critical parameter to maximize electrode performance, as limited oxygen desorption and bubble formation on the electrode can significantly increase the overpotential.[58]

Recently, initial steps were taken to replace the traditional noble-metal particles for the ORR by cheaper metals. Zhang *et al.*[59] demonstrated that cheaper silver NPs can be used as active reduction sites in the ORR: the group reported a facile, one-pot synthesis of Ag NP-decorated CNTs by reaction of acidized MWNTs with $AgNO_3$ using *in situ* photoreduced Keggin anions as reducing agent and bridging molecules. The composites showed a high electrocatalytic ORR activity due to the synergistic effect between Ag NPs and CNTs. For the POM-functionalized system, significantly increased ORR current densities were observed compared with non-functionalized CNTs.

The ORR activity of Ag NPs was substantiated in 2013, when a 2D-Ag nano-net (NN) functionalized graphene was reported as a substitution for Pt catalysts for the ORR. The group used $H_7[\beta\text{-}PMo_4{}^{V}Mo_8{}^{VI}O_{40}]$ as the reducing agent[60] (Fig. 8) to deposit an Ag nanostructure on graphene. The as-prepared composites showed high electrocatalytic ORR activity associated with the high catalytic activity of the Ag NNs and the excellent electron transfer properties of GNs reinforced by the presence of residual POM units and fragments arising from their decomposition. Compared to a Pt/C reference catalyst, the composites are cheaper and more stable and significantly lower activity losses over time were reported compared with the Pt/C reference system. The results show that oxygen reduction electrodes can already be developed based on economically viable and technologically relevant metals when combined with POMs.

3.1.4 Further applications. The versatility of the systems discussed and their potential in future applications with relevance to energy conversion and storage as well as environmental sensing and pollutant removal is briefly described here:

Jiang *et al.*[61] showed that the Pd@POM/PDDA/MWNTs system discussed earlier is not limited to the ORR but can also be used for formic acid oxidation in fuel cells. In their system, the Pd NPs supported on POM/PDDA/MWNT show homogeneous dispersion and narrow particle size distribution; it is suggested that the presence of the POMs inhibits the agglomeration of Pd NPs. In comparison, the acid-treated MWNTs feature randomly located defects, resulting in a relatively poor dispersion and aggregation of Pd NPs.

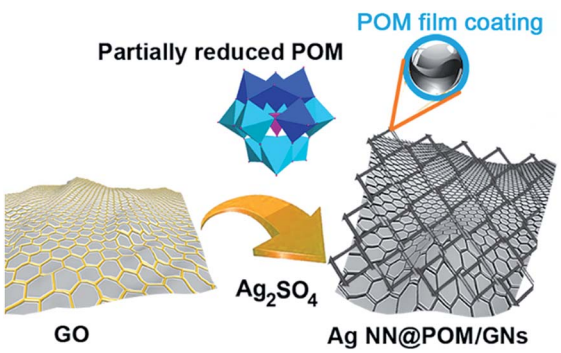

Fig. 8 Polyoxometalate-mediated large-scale synthesis of 2D Ag NN@POM/GNs composites using the mixed-valent Keggin-type POM $H_7[\beta\text{-}PMo_4{}^{V}Mo_8{}^{VI}O_{40}]$.[60]

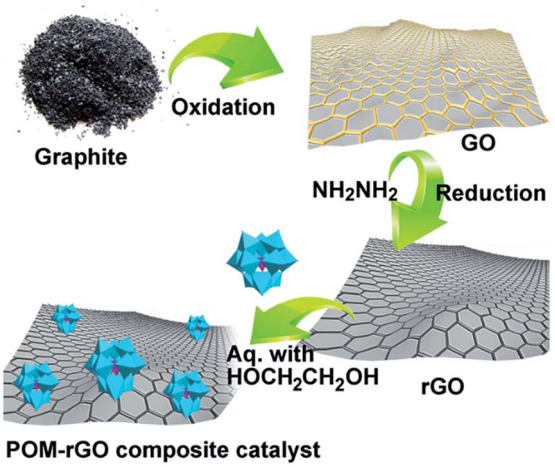

Fig. 9 Schematic representation of the fabrication of POM–rGO composite.[62] (1) Oxidation of graphite using a modified Hummer method;[63] (2) reduction of GO by hydrazine hydrate, giving rise to rGO; (3) functionalization of the rGO with Keggin-type POM anions under mild conditions giving the POM–rGO composite.

In research focused on environmental pollutants, Shanmugam *et al.*[62] showed that PMO_{12}/rGO composite is a superior catalyst for nitrite electro-oxidation compared with the two components alone and a 20-fold increase in activity compared with pure rGO was observed. It is suggested that PMo_{12} assists the graphene oxidation and results in the formation of defect sites on the GNs (Fig. 9). UV-vis and Raman spectroscopy revealed strong electron transfer interactions between the graphene sheet and POMs induced at the graphene sheet defect sites. This led to a modification of the band gap energy and resulted in a more robust catalyst material.

These initial examples demonstrate that POM-modified nanocarbons are highly robust and versatile systems which can be employed in a wide range of technologically relevant electrocatalytic reactions, so that future applications in various fields can be targeted by specific chemical modification of the POM reactivity.

3.2 Energy storage

Electrochemical energy storage is currently on of the fastest-growing fields or research involving nanostructured hybrid materials.[64,65] The most promising systems for electrochemical energy storage are (1) batteries, where energy storage and release is based on chemical redox reactions and (2) supercapacitors where energy storage is based on a combination of electrostatic charge separation (double layer capacitance) and electrochemical charge separation (pseudo-capacitance).[66,67]

Owing to their high intrinsic electron-storage capacity, their chemical tunability and high stability, POMs are ideal candidates for electrochemical energy storage.[68–70] However, as POMs

are molecular units, electronic conductivity between clusters is negligible, so in order to achieve high electronic conductivity, ideally each cluster molecule needs to be electrically linked to a conductive substrate.[71] Thus, combining redox-active POMs as electron storage sites with nano-structured carbon materials as electrical conductors with high surface area is a promising approach for the design of high-capacity energy storage systems. This section summarizes recent progress in the design of POM/CNT or POM/graphene composites as electrode materials for lithium ion batteries and supercapacitors and emphasizes key development areas where POM-based research is urgently required.

3.2.1 Lithium ion batteries. Lithium ion batteries are at the forefront of battery research due to their high specific energy density. Recently, first steps have been taken to incorporate POMs in these systems; the POMs are employed as electron storage sites, as well as electron-transfer mediators. Thus far, the investigations have been focused mainly on Keggin and/or Dawson-type clusters hybridized with CNTs or graphene.

Awaga *et al.*[28,69,70] have introduced the concept of molecular cluster batteries (MCBs) for electrochemical energy storage. Their initial studies used a nanocomposite of $(n\text{-}Bu_4N)_3[PMo_{12}O_{40}]$/SWNTs. Attachment of the cluster to the SWNTs was achieved by electrostatic interactions, as the $n\text{-}Bu_4N^+$ counter ions interacted with the SWNTs and created positive surface charges which were used to bind the anionic POM. Molecular dispersion of the POM clusters was achieved, resulting in smooth electron transfer and fast lithium-ion diffusion (Fig. 10). The material was used to assemble a cathode and a specific capacity of up to 320 mA h g^{-1} was observed. This compares favourably with a reference system of the pure identical cluster, where a specific capacity of 260 mA h g^{-1} was found, showing the effectiveness of the electrical "wiring" of the POM to the SWNTs.

Recently, Song *et al.*[29] studied new modes of chemically attaching redox-active POMs to SWNTs for improved charge-transfer. To this end, the authors developed a novel method to modify SWNTs with organo-functionalized $[SiW_{11}O_{39}]^{7-}$ clusters. Pyrene moieties were covalently attached to the cluster by silanol linkages and the functionalized clusters were bound to the SWNTs through π–π stacking, allowing the assembly of Py–SiW_{11}/SWNT/nano-composite materials (Fig. 11). Utilized as the anode material, the composite exhibits excellent performance with an initial discharge capacity of 1570 mA h g^{-1}. Over longer periods (up to 100 cycles), high discharge capacities of 580 mA h g^{-1} were maintained, significantly enhancing the capacity of non-functionalized CNTs which are in the region of 400 to 460 mA h g^{-1}. In the next step, the group currently investigates the covalent attachment of POMs to CNTs.

A different approach to maximize the electronic interactions between POM and nanocarbons was introduced by Paek *et al.*[72] The group used the ability of POMs to pillar sheets of GO and fabricated a highly ordered nanostructure composed of layered GO and Keggin-type aluminum POMs (Al_{13}). Battery tests show that Al_{13}-intercalated GO exhibits a significantly increased reversible capacity, compared with that of the pristine GO, highlighting that cluster-intercalated GO stacks are promising materials for high-capacity electrodes. Future work using tungstate or molybdate POMs as highly redox-active pillaring agents might result in further improvement of the electrode capacity.

Further work to increase the conductivity of POM/graphene composites was performed by Bubeck *et al.*[32] who developed a green method to reduce GO *via* a UV-driven photo-reduction process. H_3PW_{12} was used as photo-catalyst (Fig. 12) and also acted as an anionic surface-active molecule which increased the rGO dispersibility in water by attaching to the surface of rGO. The group found that the conductivity of the POM-modified rGO as high as 400 S m^{-1}, compared with that of hydrazine-reduced GO which is in the region of 3×10^{-6} S m^{-1} only. This result shows that the POM-assisted photo-reduction method significantly increases the electronic conjugation between GO sheets, resulting in dramatically higher electronic conductivity.

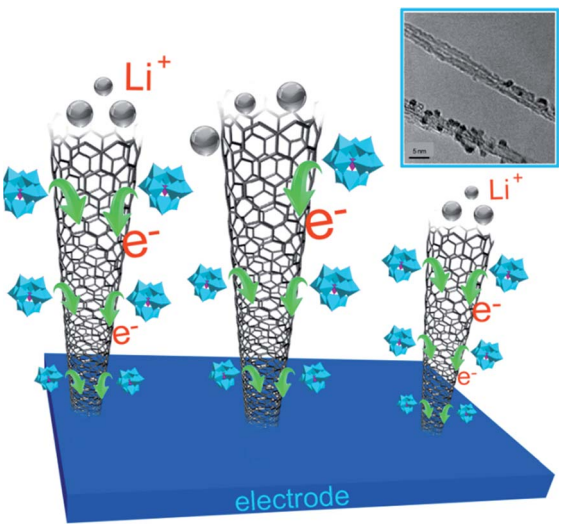

Fig. 10 Schematic illustration of a molecular cluster battery (MCB) based on POM/SWNTs composites. Well-dispersed POM clusters are attached to CNTs *via* electrostatic interactions to improve electronic conductivity and ion diffusion. Inset: TEM image of POM/SWNT hybrid materials.[28] Reproduced from ref. 28 with permission of John Wiley and Sons Publishers.

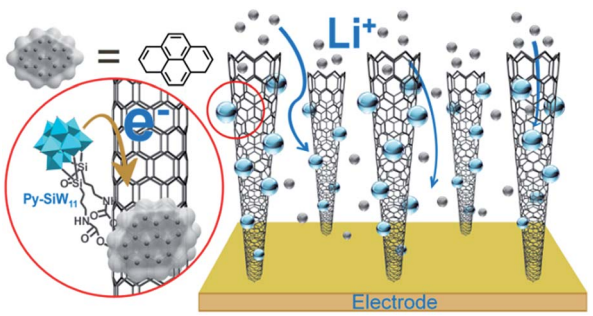

Fig. 11 Schematic illustration of the Py–PW_{11}/SWNTs/nanocomposite as anode material covalently functionalized POM clusters were attached to the SWNTs through π–π stacking interactions.[29]

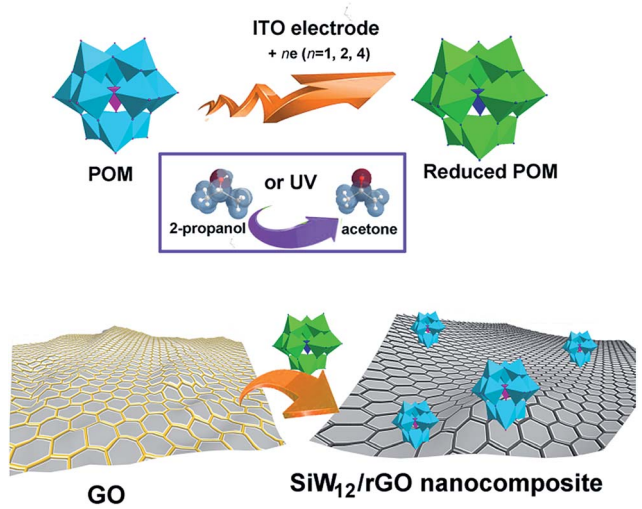

Fig. 12 Electrochemical or photochemical reduction-assisted assembly of SiW_{12}/rGO nanocomposites.[32,33] Electrochemical or photochemical reduction gives the reduced SiW_{12} cluster. Reaction with GO leads to the SiW_{12}/rGO nanocomposite where GO is reduced *in situ* by the cluster.

The initial results on POM-based battery electrodes highlight the need for highly redox-active molecular materials with chemical redox-tuneability and high cycling stability. Future work requires the interdisciplinary collaboration between POM chemists, materials chemists and battery researchers to optimize the components employed, to enable efficient electron transfer between the components by enhancing their electronic linkage and to develop strategies for device integration.

3.2.2 Supercapacitors. Carbon-based materials have been widely studied as electrode materials for supercapacitors, often giving devices with relatively low energy density.[73,74] Particularly for automotive applications the specific energy density needs to be increased. One approach is the embedding of materials capable of undergoing reversible multi-electron redox processes. The current gold-standard for supercapacitors is RuO_2 as pseudo-capacitive material, because of its fast and reversible multi-electron transfer reactions with overlapping peak potentials.[75] Recently, POMs have been suggested as chemically and economically viable replacements for the noble metal oxide due their unique redox chemistry.

Groundbreaking studies by Gómez-Romero *et al.*[76] used Cs–PMo_{12}/CS/CNTs hybrid materials obtained by immobilizing Cs-containing POM anions on cationic, chitosan (CS) functionalized CNTs as composite electrodes in symmetric supercapacitors. Their initial studies showed that the composites feature high capacitance and good stability was observed over 500 charge–discharge cycles, suggesting that further development of this device configuration is promising.

Lian *et al.*[30,77] demonstrated that facile LbL assembly techniques can be used to access supercapacitors. The group used a 3-layer LbL assembly based on MWNTs, PDDA and two types of pseudo-capacitive POMs, $[SiMo_{12}O_{40}]^{4-}$ ($SiMo_{12}$) and $[PMo_{12}O_{40}]^{3-}$ (PMo_{12}) (Fig. 13). The composites achieved an up to four-fold increase in area specific capacitance when compared with the double layer capacitance of non-functionalized MWNTs. The group subsequently extended the research[78] by adding $[PV_2Mo_{10}]^{5-}$ (PV_2Mo_{10}) into the LbL deposition. The results showed that a dual-layer coating by PMo_{12} and PV_2Mo_{10} on MWNTs showed a collective contribution of both active layers, increasing not only charge storage capacity but also the voltage window.

The LbL supercapacitor assembly was further extended by Kulesza *et al.*[79] who prepared a composite by depositing the Dawson anion $[P_2VW_{17}O_{62}]^{8-}$ onto MWNTs. The materials feature a high specific capacitance of 82 F g^{-1} (at the charging/discharging current of 200 mA g^{-1}) compared with bare CNTs where the specific capacitance under identical conditions was only 50 F g^{-1}. The results confirm that the LbL technique is a simple and effective tool for developing thin, nano-scale POM/CNT multilayer coatings to enhance the capacitance without sacrificing electric conductivity. Further, the studies show that by chemical modification of the POM components, significant changes in supercapacitor performance can be achieved, highlighting the urgent need for more detailed studies where other, non-prototype POMs are used in device fabrication.

3.2.3 Other electrochemical devices. The versatility of LbL-assembled POM–nanocarbon devices was further exploited by Müllen *et al.*[34] who reported that GO nanosheets and $H_3PW_{12}O_{40}$ can be assembled into multilayer films *via* electrostatic LbL assembly. Under UV irradiation, a POM-based photoreduction of GO to rGO is observed. The obtained films were used to fabricate field effect transistors, which exhibited typical ambipolar features and good transport properties for both holes and electrons. The on/off ratios and the charge carrier mobilities of the transistors depend on the number of deposited layers and were easily adjustable. Furthermore, efficient microelectrodes for photo-detector devices could be produced using photomasks to form conductive rGO patterns within the composite films.

A similar LbL approach allowed Xu *et al.*[80] to fabricate electrochromic nanocomposite films containing $[P_2W_{18}O_{62}]^{6-}$, CNTs, and chitosan (CS). The electrochromic properties of the composite were improved by CNT incorporation, resulting in

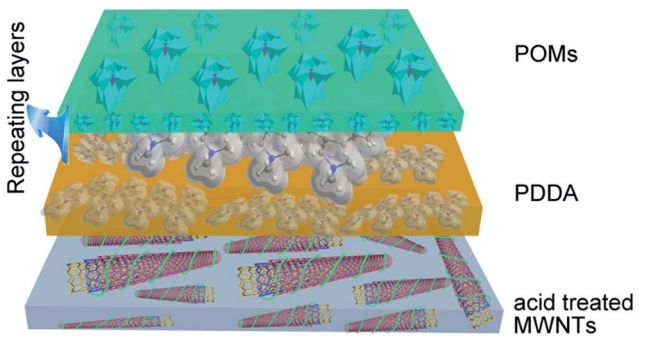

Fig. 13 Schematic representation of the 3-layer LbL deposition using MWNTs, PDDA and POM.[30] MWNTs are prepared as a thin film and acidized using nitric acid. A second layer of PDDA is dip-coated onto the MWNT film. Then, the POM layer is dip-coated onto the cationic PDDA film, giving the final composite.

superior electrochromic performance compared to the non-hybridized reference, suggesting that the composite can offer longer operational lifetimes when used in electrochromic devices.

In summary, this section illustrates the broad versatility and wide application range of POM-modified nanocarbon materials. However, one striking feature of the results described is the fact that research is almost exclusively focused on the prototype Keggin and Dawson anions. Therefore there is a tremendous opportunity for the use of the large number of other accessible POM anions which could easily be accessed and deposited on nanocarbons by close collaboration between researchers from both fields. As such, it can be envisaged that the coming years will provide significant leaps forward in developing materials where selective chemical modification of the POMs is used to target specific redox activity or catalytic activity in a composite material.

3.3 Sensors for environmental pollutants

The ability of POMs to undergo reversible multi-electron redox-processes makes them interesting for amperometric sensor applications, such as detection of redox-active industrial and agricultural pollutants, *e.g.* nitrate,[81] bromate,[82] chlorate,[83] iodate,[84] and hydrogen peroxide.[85–87] To read out the sensing information and to maximize amperometric response, the POMs need to be anchored or immobilized on conductive substrates while at the same time maintaining molecular dispersion to reach low analyte detection limits. Therefore, CNTs and graphene are ideal substrates for this purpose.[88–90] Herein, a series of POM–CNTs and POM–graphene composites as sensor electrodes or devices are discussed, their limitations are highlighted and future research directions are proposed.

3.3.1 Hydrogen peroxide sensors. Hydrogen peroxide (H_2O_2) is industrially used as anti-bacterial and sterilizing agent.[91] In addition, peroxides are released from many other industrial processes, and their environmental release needs to be strictly controlled.[92] To this end, Salimi *et al.*[93] developed a three component electrochemical peroxide sensor: the group modified glassy carbon (GC) electrodes with SWNTs, $SiMo_{12}$ and the copper complex $[Cu(bpy)_2]Br$. The copper complex and POM were irreversibly and strongly adsorbed onto the GC electrode. Over a wide pH-range, the electrode showed three reversible redox couples for the POM and one redox couple for the Cu-complex. Compared with a non-POM functionalized reference electrode (based on a GC electrode modified with SWNTs and $[Cu(bpy)_2]Br_2$ only), the POM-modified system showed stable voltammetric response and gave excellent electrocatalytic activity towards H_2O_2 reduction (bromate reduction was also reported) at low over-potentials. The system was able to detect nanomolar concentrations of hydrogen peroxide and bromate, highlighting the sensitivity which is associated with the highly dispersed POMs on the nanostructured conductive substrate.

The group of Gorton *et al.* used a simple dip-coating procedure to assemble a robust and stable film composed of the ionic liquid $[C_8Py][PF_6]$ and PMo_{12} on MWNT-modified GC electrodes.[94] Efficient H_2O_2 and iodate detection at low over-potentials was found together with low detection limits, high sensitivity, short response time (<2 s) and wide linear concentration range, illustrating that in principle the sensors can be assembled in the field and used for *in situ* pollutant detection. The use of the ionic liquid might have additional benefits as their high conductivity presumably contributes to the electron transfer between POM and MWNT substrate.

3.3.2 Iodate and bromate sensors. Iodate and bromate are environmental pollutants and suspected carcinogens formed *e.g.* in drinking water upon ozone treatment.[95] *In situ* detection is therefore of high technological interest. The problem was addressed by Chen *et al.* who developed an amperometric bromate sensor based on a PMo_{12}/MWNTs/composite film.[82] The authors reported low detection limits (0.5 μM), high sensitivity (760.9 μA mM^{-1} cm^{-2}), short response times (<2 s) and wide linear range (5 μM to 15 mM). This research was expanded by Dong *et al.*[96] who investigated the effects of a series of Keggin and Dawson POMs as redox-active sites together with different electrode assembly procedures to better understand how to maximise sensor performance. To this end, a series of carbon nanotube paste (CNTP) electrodes based on purified MWNTs and methyl silicone oil were developed. The most successful system was based on the Dawson-anion P_2Mo_{18} for which effective electrocatalytic reduction of bromate and iodate was observed. In an extension of this work, multilayer films of $(P_2Mo_{18}/PDDA)_n$ were assembled on CNTP electrodes using the LbL technique and comparative studies showed higher electrocatalytic activity for the LbL-assembled composites compared with the composite materials fabricated by direct electrostatic assembly.

Work on Dawson-modified sensors was further expanded by Xu *et al.*[97] who reported a modified electrode where CNTs were dispersed in polycationic chitosan films which were then used to electrostatically immobilize Dawson anions P_2W_{18}. Electrochemical studies demonstrated that the P_2W_{18}/CS/CNT electrode exhibits fast response and good electrocatalytic activity for the reduction of peroxodisulfate and iodate anions and it was reported that the sensor works under acidic conditions also, broadening its applicability under industrial conditions.

In summary, the studies illustrate that the choice of cluster anion as well as the assembly method is crucial and emphasizes that future electrode development needs to be driven by inter-disciplinary research, ranging from molecular materials design to nano- and microstructuring of the composites.

In addition, it should be briefly noted that POM/nanocarbon composites have been used for the detection of a large number of other organic and inorganic analytes, including antimony,[98] sulfite,[99] glucose,[100] dopamine[101] and ascorbic acid.[102]

3.3.3 Future developments and applications. As briefly described earlier, the future development of POM/nanocarbon materials rests on several pillars. One obvious and to the authors highly promising approach is to investigate non-prototype POMs where novel reactivity, higher stability and different reactivity can be expected. To this end, an

interdisciplinary approach is urgently required where target systems (*i.e.* electrocatalytic substrates, industrial pollutants, *etc.*) are determined and POMs which can interact with these targets are identified and combined with nanocarbon materials. This combination of materials by itself is still challenging and novel approaches for the assembly of POM/nanocarbon composites are required to access electrode materials with high stability and reactivity.

The importance of the method of electrode assembly has been discussed in several examples (see above). One highly innovative approach to POM/nanocarbon layered electrodes which might be used for large-scale, automated fabrication has recently been presented by Shen *et al.*[103] The group used a combined LbL-inkjet-printing approach to assemble layered PW_{12}/rGO composites (Fig. 14). The composite thin film showed linear, uniform and regular layer-by-layer growth. Under UV-irradiation, a POM-driven photo-reduction led to the conversion of GO to rGO, and the materials were used as highly responsive dopamine sensors.

A further promising field of research is the development of photoactive electrodes for use in photocatalysis or photovoltaics:[104] initial work by Zhang *et al.*[105] showed the versatility of the approach: the authors assembled an Au NPs@POM/CNT tri-component composite (Fig. 15) which was employed in photo-oxidative test reactions and showed significant enhancement on the photocatalytic degradation of Rhodamine B under visible light irradiation. The mechanism proposed is a visible light-induced, POM-mediated electron transfer from the Au NPs to CNTs resulting in oxidative degradation of organic pollutants.

In contrast, significantly lower activity was observed for the bi-component composite Au NPs@POM, where faster charge recombination was observed due to the close proximity between POM and Au NPs. In the tri-component system, the charges can easily be transferred to the CNTs, resulting in a remarkable synergistic enhancement of the photocatalytic activity. These initial studies clearly demonstrate the potential of using POMs not only as homogeneous photocatalysts but also as a component in composite materials with enhanced charge transfer properties.

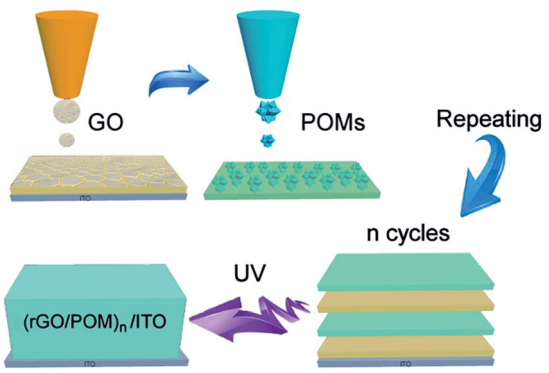

Fig. 14 Scheme of $(rGO/POM)_n$ multilayer film production by LbL fabrication using inkjet printing.[103] Repeated printing of GO and POM layers gives access to multilayer assemblies. Photoreduction of the films using UV irradiation gives the $(rGO/POM)_n$ multilayer film.

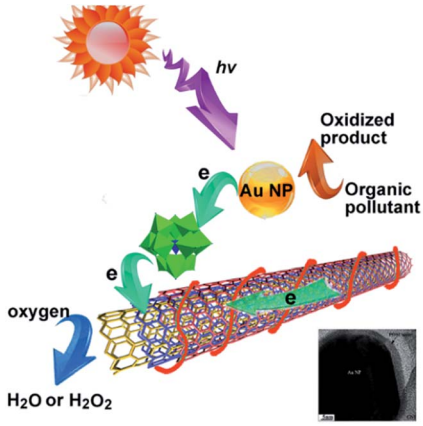

Fig. 15 The photocatalytic mechanism of Au NP@POM/CNT tri-component nanocomposites. Inset: HR-TEM image of Au NP attached on CNTs.[105] Reproduced from ref. 104 with permission of Royal Society of Chemistry Publishers.

4. Conclusions and outlook

In summary, we discuss the design, synthesis and reactivity of novel POM/nanocarbon composite materials based on POM-functionalized carbon nanotubes or graphene. Their use as efficient electrocatalysts, electrodes for Li-ion batteries, supercapacitors and sensors is highlighted and particular focus is put on their improved performance compared with relevant state-of-the-art reference systems. In addition, we focus on the discussion of potential optimization routes such as the development of new of covalent and non-covalent linkage modes between POMs and nanocarbons as well as the need to gain further understanding of the effects of different composite fabrication routes on the material properties. As nanocarbon materials become more widely available at low cost, it can be envisaged that strongly coupled POM/nanocarbon composites will find applications in technological electrochemical devices.

However, future developments for POM/nanocarbon composites are by no means limited to the above areas and in the outlook section, we highlight several research themes where POM/nanocarbon composites can address important technological challenges. Therefore, joint projects which bring together the expertise of polyoxometalate chemists, nanocarbon specialists and device fabrication experts can in future lead to real-life devices built from self-assembled POM and nanocarbon components.

Abbreviations

AA	Ascorbic acid
Al_{13}	$[AlO_4Al_{12}(OH)_{24}(H_2O)_{12}]^{7+}$
CNTP	Carbon nanotube paste
CNT	Carbon nanotube
CS	Chitosan
$Cs–PMo_{12}$	$Cs_3PMo_{12}O_{40}$
CV	Cyclic voltammogram

DMFC	Direct methanol fuel cell
ESA	Electrochemical surface area
GC/GCE	Glassy carbon/glassy carbon electrode
GNs	Graphene nanosheets
GO	Graphene oxide
HER	Hydrogen evolution reaction
HR-TEM	High resolution transmission electron microscopy
IL	Ionic liquid
ITO	Indium tin oxide
LbL	Layer-by-layer
MCBs	Molecular cluster batteries
MWNTs	Multi-walled carbon nanotubes
NN	Nano-net
NPs	Nanoparticles
OEAs	Oxygen-evolving anodes
ORR	Oxygen reduction reaction
PDDA	Poly(diallyldimethylammonium chloride)
PEI	Poly(ethyleneimine)
PMo_{12}	$[PMo_{12}O_{40}]^{3-}$
POMs	Polyoxometalates
PTFE	Polytetrafluoroethylene
PV_2Mo_{10}	$[PV_2Mo_{10}O_{40}]^{5-}$
PW_{12}	$[PW_{12}O_{40}]^{3-}$
P_5W_{30}	$[NaP_5W_{30}O_{110}]^{14-}$
Py	Pyrene
rGO	Reduced graphene oxide
Ru4(POM)	$Ru_4(H_2O)_4(\mu\text{-}O)_4(\mu\text{-}OH)_2(\gamma\text{-}SiW_{10}O_{36})_2$
$SiMo_{12}$	$[SiMo_{12}O_{40}]^{4-}$
SiW_{12}	$[SiW_{12}O_{40}]^{4-}$
TBA	Tetrabutylammonium
TEM	Transmission electron microscopy
TOF	Turnover frequency
UV	Ultraviolet
UV-vis	Ultraviolet-visible
WOC	Water oxidation catalyst
$[C_8Py][PF_6]$	*n*-Octylpyridinium hexafluorophosphat
$[Ru(bpy)(tpy)Cl]^+$	[Ru(2,2′-bipyridine) (2,2′,2″)-terpyridineCl]$^+$

Acknowledgements

Financial support from National Basic Research Program of China (973 program, 2014CB932104) and National Science Foundation of China (21222104), the Fundamental Research Funds for the Central Universities (RC1302) and the Program for Changjiang Scholars and Innovative Research Team in University are kindly acknowledged. The authors acknowledge financial support from Beijing Engineering Center for Hierarchical Catalysts, Ulm University and the Deutsche Forschungsgemeinschaft DFG (STR1164/4-1).

Notes and references

1 A. C. Dillon, *Chem. Rev.*, 2010, **110**, 6856–6872.
2 M. S. Whittingham, *Chem. Rev.*, 2004, **104**, 4271–4302.
3 M. V. Reddy, G. V. Subba Rao and B. V. R. Chowdari, *Chem. Rev.*, 2013, **113**, 5364–5457.
4 D. S. Su, S. Perathoner and G. Centi, *Chem. Rev.*, 2013, **113**, 5782–5816.
5 G. Lota, K. Fic and E. Frackowiak, *Energy Environ. Sci.*, 2011, **4**, 1592–1605.
6 F. F. Bamoharram, *Synth. React. Inorg., Met.-Org., Nano-Met. Chem.*, 2011, **41**, 893–922.
7 Y.-F. Song and R. Tsunashima, *Chem. Soc. Rev.*, 2012, **41**, 7384–7402.
8 M. Quintana, A. M. López, S. Rapino, F. M. Toma, M. Iurlo, M. Carraro, A. Sartorel, C. Maccato, X. Ke, C. Bittencourt, T. Da Ros, G. Van Tendeloo, M. Marcaccio, F. Paolucci, M. Prato and M. Bonchio, *ACS Nano*, 2012, **7**, 811–817.
9 A. Müller, F. Peters, M. T. Pope and D. Gatteschi, *Chem. Rev.*, 1998, **98**, 239–272.
10 A. Dolbecq, E. Dumas, C. R. Mayer and P. Mialane, *Chem. Rev.*, 2010, **110**, 6009–6048.
11 S. Omwoma, W. Chen, R. Tsunashima and Y.-F. Song, *Coord. Chem. Rev.*, 2014, **258–259**, 58–71.
12 R. L. McCreery, *Chem. Rev.*, 2008, **108**, 2646–2687.
13 D. A. C. Brownson, D. K. Kampouris and C. E. Banks, *Chem. Soc. Rev.*, 2012, **41**, 6944–6976.
14 C. Xu, B. Xu, Y. Gu, Z. Xiong, J. Sun and X. S. Zhao, *Energy Environ. Sci.*, 2013, **6**, 1388–1414.
15 E. S. Andreiadis, P.-A. Jacques, P. D. Tran, A. Leyris, M. Chavarot-Kerlidou, B. Jousselme, M. Matheron, J. Pecaut, S. Palacin, M. Fontecave and V. Artero, *Nat. Chem.*, 2013, **5**, 6–7.
16 Y. Liang, Y. Li, H. Wang and H. Dai, *J. Am. Chem. Soc.*, 2013, **135**, 2013–2036.
17 M. Pumera, *Chem. Rec.*, 2009, **9**, 211–223.
18 R. Tsunashima, Y. Iwamoto, Y. Baba, C. Kato, K. Ichihashi, S. Nishihara, K. Inoue, K. Ishiguro, Y.-F. Song and T. Akutagawa, *Angew. Chem., Int. Ed.*, 2014, **53**, 11228–11231.
19 J. P. Tessonnier, S. Goubert-Renaudin, S. Alia, Y. S. Yan and M. A. Barteau, *Langmuir*, 2013, **29**, 393–402.
20 F. M. Toma, A. Sartorel, M. Iurlo, M. Carraro, P. Parisse, C. Maccato, S. Rapino, B. R. Gonzalez, H. Amenitsch, T. Da Ros, L. Casalis, A. Goldoni, M. Marcaccio, G. Scorrano, G. Scoles, F. Paolucci, M. Prato and M. Bonchio, *Nat. Chem.*, 2010, **2**, 826–831.
21 S. Li, X. Yu, G. Zhang, Y. Ma, J. Yao and P. de Oliveira, *Carbon*, 2011, **49**, 1906–1911.
22 R. Liu, S. Li, X. Yu, G. Zhang, S. Zhang, J. Yao and L. Zhi, *J. Mater. Chem.*, 2012, **22**, 3319–3322.
23 R. Liu, S. Li, X. Yu, G. Zhang, S. Zhang, J. Yao, B. Keita, L. Nadjo and L. Zhi, *Small*, 2012, **8**, 1398–1406.
24 A. Proust, R. Thouvenot and P. Gouzerh, *Chem. Commun.*, 2008, 1837–1852.
25 A. Proust, B. Matt, R. Villanneau, G. Guillemot, P. Gouzerh and G. Izzet, *Chem. Soc. Rev.*, 2012, **41**, 7605–7622.
26 W. Chen, L. Huang, J. Hu, T. Li, F. Jia and Y.-F. Song, *Phys. Chem. Chem. Phys.*, 2014, **16**, 19668–19673.
27 N. Kawasaki, H. Wang, R. Nakanishi, S. Hamanaka, R. Kitaura, H. Shinohara, T. Yokoyama, H. Yoshikawa and K. Awaga, *Angew. Chem.*, 2011, **123**, 3533–3536.

28 N. Kawasaki, H. Wang, R. Nakanishi, S. Hamanaka, R. Kitaura, H. Shinohara, T. Yokoyama, H. Yoshikawa and K. Awaga, *Angew. Chem., Int. Ed.*, 2011, **50**, 3471–3474.
29 D. Ma, L. Liang, W. Chen, H. Liu and Y.-F. Song, *Adv. Funct. Mater.*, 2013, **23**, 6100–6105.
30 T. Akter, K. Hu and K. Lian, *Electrochim. Acta*, 2011, **56**, 4966–4971.
31 Y. Xiang, S. Lu and S. P. Jiang, *Chem. Soc. Rev.*, 2012, **41**, 7291–7321.
32 H. Li, S. Pang, X. Feng, K. Müllen and C. Bubeck, *Chem. Commun.*, 2010, **46**, 6243–6245.
33 S. Wang, H. Li, S. Li, F. Liu, D. Wu, X. Feng and L. Wu, *Chem.–Eur. J.*, 2013, **19**, 10895–10902.
34 H. Li, S. Pang, S. Wu, X. Feng, K. Müllen and C. Bubeck, *J. Am. Chem. Soc.*, 2011, **133**, 9423–9429.
35 M. T. M. Koper, *Nat. Chem.*, 2013, **5**, 255–256.
36 R. Subbaraman, D. Tripkovic, D. Strmcnik, K.-C. Chang, M. Uchimura, A. P. Paulikas, V. Stamenkovic and N. M. Markovic, *Science*, 2011, **334**, 1256–1260.
37 C. Bianchini and P. K. Shen, *Chem. Rev.*, 2009, **109**, 4183–4206.
38 D. Simonsson, *Chem. Soc. Rev.*, 1997, **26**, 181–189.
39 H. J. Lv, Y. V. Geletii, C. C. Zhao, J. W. Vickers, G. B. Zhu, Z. Luo, J. Song, T. Q. Lian, D. G. Musaev and C. L. Hill, *Chem. Soc. Rev.*, 2012, **41**, 7572–7589.
40 A. Sartorel, M. Bonchio, S. Campagna and F. Scandola, *Chem. Soc. Rev.*, 2013, **42**, 2262–2280.
41 M. W. N. Kanan and G. Daniel, *Science*, 2008, **321**, 1072–1075.
42 F. M. Toma, A. Sartorel, M. Iurlo, M. Carraro, S. Rapino, L. Hoober-Burkhardt, T. Da Ros, M. Marcaccio, G. Scorrano, F. Paolucci, M. Bonchio and M. Prato, *ChemSusChem*, 2011, **4**, 1447–1451.
43 A. Ambrosi, C. K. Chua, A. Bonanni and M. Pumera, *Chem. Rev.*, 2014, **114**, 7150–7188.
44 S.-X. Guo, Y. Liu, C.-Y. Lee, A. M. Bond, J. Zhang, Y. V. Geletii and C. L. Hill, *Energy Environ. Sci.*, 2013, **6**, 2654–2663.
45 Q. S. Yin, J. M. Tan, C. Besson, Y. V. Geletii, D. G. Musaev, A. E. Kuznetsov, Z. Luo, K. I. Hardcastle and C. L. Hill, *Science*, 2010, **328**, 342–345.
46 H. Liu, C. Song, L. Zhang, J. Zhang, H. Wang and D. P. Wilkinson, *J. Power Sources*, 2006, **155**, 95–110.
47 W. Li, C. Liang, W. Zhou, J. Qiu, Z. Zhou, G. Sun and Q. Xin, *J. Phys. Chem. B*, 2003, **107**, 6292–6299.
48 D. Pan, J. Chen, W. Tao, L. Nie and S. Yao, *Langmuir*, 2006, **22**, 5872–5876.
49 M. H. Seo, S. M. Choi, H. J. Kim, J. H. Kim, B. K. Cho and W. B. Kim, *J. Power Sources*, 2008, **179**, 81–86.
50 D. M. Han, Z. P. Guo, R. Zeng, C. J. Kim, Y. Z. Meng and H. K. Liu, *Int. J. Hydrogen Energy*, 2009, **34**, 2426–2434.
51 Z. Cui, C. M. Li and S. P. Jiang, *Phys. Chem. Chem. Phys.*, 2011, **13**, 16349–16357.
52 X. Jin, B. He, J. Miao, J. yuan, Q. Zhang and L. Niu, *Carbon*, 2012, **50**, 3083–3091.
53 S. B. Adler, *Chem. Rev.*, 2004, **104**, 4791–4844.
54 Z. Liu, F. Peng, H. Wang, H. Yu, W. Zheng and J. Yang, *Angew. Chem., Int. Ed.*, 2011, **50**, 3257–3261.
55 Y. Kang, X. Ye, J. Chen, Y. Cai, R. E. Diaz, R. R. Adzic, E. A. Stach and C. B. Murray, *J. Am. Chem. Soc.*, 2012, **135**, 42–45.
56 M. Shao, K. Shoemaker, A. Peles, K. Kaneko and L. Protsailo, *J. Am. Chem. Soc.*, 2010, **132**, 9253–9255.
57 D. Wang, S. Lu and S. P. Jiang, *Chem. Commun.*, 2010, **46**, 2058–2060.
58 Y. Suo, L. Zhuang and J. Lu, *Angew. Chem., Int. Ed.*, 2007, **46**, 2862–2864.
59 R. Liu, S. Li, X. Yu, G. Zhang, Y. Ma and J. Yao, *J. Mater. Chem.*, 2011, **21**, 14917–14924.
60 R. Liu, X. Yu, G. Zhang, S. Zhang, H. Cao, A. Dolbecq, P. Mialane, B. Keita and L. Zhi, *J. Mater. Chem. A*, 2013, **1**, 11961–11969.
61 Z. Cui, P. J. Kulesza, C. M. Li, W. Xing and S. P. Jiang, *Int. J. Hydrogen Energy*, 2011, **36**, 8508–8517.
62 Y. Kim and S. Shanmugam, *ACS Appl. Mater. Interfaces*, 2013, **5**, 12197–12204.
63 W. S. Hummers and R. E. Offeman, *J. Am. Chem. Soc.*, 1958, **80**, 1339.
64 Y. Zhu, S. Murali, M. D. Stoller, K. J. Ganesh, W. Cai, P. J. Ferreira, A. Pirkle, R. M. Wallace, K. A. Cychosz, M. Thommes, D. Su, E. A. Stach and R. S. Ruoff, *Science*, 2011, **332**, 1537–1541.
65 B. L. Ellis, P. Knauth and T. Djenizian, *Adv. Mater.*, 2014, **26**, 3368–3397.
66 K. Xie and B. Wei, *Adv. Mater.*, 2014, **26**, 3592–3617.
67 Q. Lu, J. G. Chen and J. Q. Xiao, *Angew. Chem., Int. Ed.*, 2013, **52**, 1882–1889.
68 J. M. Poblet, X. Lopez and C. Bo, *Chem. Soc. Rev.*, 2003, **32**, 297–308.
69 Y. Nishimoto, D. Yokogawa, H. Yoshikawa, K. Awaga and S. Irle, *J. Am. Chem. Soc.*, 2014, **136**, 9042–9052.
70 H. Wang, S. Hamanaka, Y. Nishimoto, S. Irle, T. Yokoyama, H. Yoshikawa and K. Awaga, *J. Am. Chem. Soc.*, 2012, **134**, 4918–4924.
71 H.-Y. Chen, G. Wee, R. Al-Oweini, J. Friedl, K. S. Tan, Y. Wang, C. L. Wong, U. Kortz, U. Stimming and M. Srinivasan, *ChemPhysChem*, 2014, **15**, 2162–2169.
72 H. J. Yeo, Y. Paik, S.-M. Paek and I. Honma, *J. Phys. Chem. Solids*, 2012, **73**, 1417–1419.
73 M. F. L. De Volder, S. H. Tawfick, R. H. Baughman and A. J. Hart, *Science*, 2013, **339**, 535–539.
74 Q. Meng, H. Wu, Y. Meng, K. Xie, Z. Wei and Z. Guo, *Adv. Mater.*, 2014, **26**, 4100–4106.
75 H. Over, *Chem. Rev.*, 2012, **112**, 3356–3426.
76 A. Cuentas-Gallegos, R. Martinez-Rosales, M. Baibarac, P. Gómez-Romero and M. E. Rincon, *Electrochem. Commun.*, 2007, **9**, 2088–2092.
77 G. Bajwa, T. Akter and K. Lian, *ECS Trans.*, 2011, **35**, 31–37.
78 G. Bajwa, M. Genovese and K. Lian, *ECS J. Solid State Sci. Technol.*, 2013, **2**, M3046–M3050.
79 M. Sosnowska, M. Goral-Kurbiel, M. Skunik-Nuckowska, R. Jurczakowski and P. Kulesza, *J. Solid State Electrochem.*, 2013, **17**, 1631–1640.

80 S. Liu, L. Xu, F. Li, W. Guo, Y. Xing and Z. Sun, *Electrochim. Acta*, 2011, **56**, 8156–8162.
81 P. Wang, X. Wang, L. Bi and G. Zhu, *Analyst*, 2000, **125**, 1291–1294.
82 Z. Li, J. Chen, D. Pan, W. Tao, L. Nie and S. Yao, *Electrochim. Acta*, 2006, **51**, 4255–4261.
83 A. Manivel, R. Sivakumar, S. Anandan and M. Ashokkumar, *Electrocatalysis*, 2012, **3**, 22–29.
84 Y. Li, W. Bu, L. Wu and C. Sun, *Sens. Actuators, B*, 2005, **107**, 921–928.
85 N. Anwar, M. Vagin, F. Laffir, G. Armstrong, C. Dickinson and T. McCormac, *Analyst*, 2012, **137**, 624–630.
86 X. Wang, H. Zhang, E. Wang, Z. Han and C. Hu, *Mater. Lett.*, 2004, **58**, 1661–1664.
87 M. Zhou, L. Guo, F. Lin and H. Liu, *Anal. Chim. Acta*, 2007, **587**, 124–131.
88 J. J. Gooding, *Electrochim. Acta*, 2005, **50**, 3049–3060.
89 I. Dumitrescu, P. R. Unwin and J. V. Macpherson, *Chem. Commun.*, 2009, 6886–6901.
90 M. Pumera, *Chem.–Eur. J.*, 2009, **15**, 4970–4978.
91 L. K. Charkoudian, D. M. Pham and K. J. Franz, *J. Am. Chem. Soc.*, 2006, **128**, 12424–12425.
92 W. A. Pryor, B. Das and D. F. Church, *Chem. Res. Toxicol.*, 1991, **4**, 341–348.
93 A. Salimi, A. Komi, R. Hallaj, R. Khoshnavazi and H. Hadadzadeh, *Anal. Chim. Acta*, 2009, **635**, 63–70.
94 B. Haghighi, H. Hamidi and L. Gorton, *Electrochim. Acta*, 2010, **55**, 4750–4757.
95 Y. Zhang, F. Wen, Y. Jiang, L. Wang, C. Zhou and H. Wang, *Electrochim. Acta*, 2014, **115**, 504–510.
96 J. Qu, X. Zou, B. Liu and S. Dong, *Anal. Chim. Acta*, 2007, **599**, 51–57.
97 W. Guo, L. Xu, F. Li, B. Xu, Y. Yang, S. Liu and Z. Sun, *Electrochim. Acta*, 2010, **55**, 1523–1527.
98 A. Salimi, A. Korani, R. Hallaj and R. Khoshnavazi, *Electroanalysis*, 2008, **20**, 2509–2517.
99 A. Salimi, A. Korani, R. Hallaj, S. Soltanian and H. Hadadzadeh, *Thin Solid Films*, 2010, **518**, 5304–5310.
100 X. Li, Q. Y. Zhu, S. F. Tong, W. Wang and W. B. Song, *Sens. Actuators, B*, 2009, **136**, 444–450.
101 Y. Ling, Q. Huang, M. Zhu, D. Feng, X. Li and Y. Wei, *J. Electroanal. Chem.*, 2013, **693**, 9–15.
102 W. Zhang, D. Du, D. Gunaratne, R. Colby, Y. Lin and J. Laskin, *Electroanalysis*, 2014, **26**, 178–183.
103 H. Zhang, A. Xie, Y. Shen, L. Qiu and X. Tian, *Phys. Chem. Chem. Phys.*, 2012, **14**, 12757–12763.
104 C. Streb, *Dalton Trans.*, 2012, **41**, 1651–1659.
105 S. Li, X. Yu, G. Zhang, Y. Ma, J. Yao, B. Keita, N. Louis and H. Zhao, *J. Mater. Chem.*, 2011, **21**, 2282–2287.